Published in final edited form as:
Nucl Med Biol. 2008 January ; 35(1): 43–52.

(*R*)-*N*-Methyl-3-(3-^{125}I-pyridin-2-yloxy)-3-phenylpropan-1-amine ([^{125}I]PYINXT) : a novel probe for norepinephrine transporters (NET)

B. Lakshmi[1], **M-P. Kung**[1], **B. Lieberman**[1], **J. Zhao**[3], **R. Waterhouse**[3], and **H.F.Kung**[1,2]

1*Department of Radiology, University of Pennsylvania, Philadelphia, Pennsylvania 19104*

2*Department of Pharmacology, University of Pennsylvania, Philadelphia, Pennsylvania 19104*

3*Department of Psychiatry, Columbia University, NYC, NY10032*

Abstract

Alterations in the serotonin and norepinephrine neuronal functions have been observed in patients with major depression. Several antidepressants bind to both serotonin transporters (SERT) and norepinephrine transporters (NET). The ability to image NET in the human brain would be a useful step toward understanding how alterations in NET relate to disease. In this study, we report the synthesis and characterization of a new series of derivatives of iodo-nisoxetine (INXT), a known radioiodinated probe. The most promising, (*R*)-*N*-methyl-3-(3-iodopyridin-2-yloxy)-3-phenylpropylamine **(**PYINXT) **9**, displayed a high and saturable binding to NET with a K_d value of 0.53 ± 0.03 nM. Biodistribution studies of [^{125}I]PYINXT in rats showed moderate initial brain uptake (0.54 %dose/organ at 2 min) with a relatively fast washout from the brain (0.16 %dose/organ at 2 hr) as compared to [^{125}I]INXT, **7**. The hypothalamus (a NET rich region) to striatum (a region devoid of NET) ratio was found to be 2.14 at 4 hr post i.v. injection. The preliminary results suggest that this improved iodinated ligand, when labeled with ^{123}I, may be useful for mapping NET binding sites with SPECT in the living human brain.

1. Introduction

The norepinephrine transporters (NET) are transmembrane proteins located presynaptically to the noradrenergic neurons. These transporters play a critical role in noradrenergic neurotransmission by regulating the amount of norepinephrine in the synaptic cleft via reuptake mechanism [1,2]. A reduction in the level of NE in the synapse appears to down regulate the level of NET [3]. Recent research has clearly demonstrated a close association between the changes in the distribution of NET in the human brain and various diseases including CNS disorders like depression [4] attention deficit hyperactivity disorder (ADHD) [5,6] and Alzheimer's disease [7]. Non-invasive imaging with highly selective radiolabeled probes would allow us to monitor and quantify the effect of treatment (drug occupancy) or the lack thereof on NET.

*CORRESPONDING AUTHOR ADDRESS: Hank F. Kung, Ph.D., Department of Radiology, University of Pennsylvania, 3700 Market Street, Room 305, Philadelphia, PA 19104. Tel: (215) 662-3096, Fax: (215) 349-5035, e-mail: kunghf@sunmac.spect.upenn.edu.

It has been difficult to image NET with single photon emission computed tomography (SPECT) or positron emission tomography (PET) because of the lack of selective radiotracers that display good *in vivo* kinetics. An ideal radiopharmaceutical for mapping NET binding sites in the brain should meet most of the following criteria: a) high binding affinity to NET: K_i < 1 nM; b) high binding selectivity: K_i for other sites > 100 nM; c) easily labeled for imaging; d) good initial brain uptake (> 0.5% dose/organ at 2 min post-iv injection) and high target to non-target ratio (> 2); e) *in vivo* stability; f) distinctive NET-specific labeling illustrated by *ex vivo* autoradiography of rat brain sections [8].

Up to this point, the most promising NET specific radiotracer has been a methyl derivative of reboxetine, (*S,S*)-[^{11}C]-(*α*-(2-methoxyphenoxy)benzyl)morpholine (MeNER) **2** (Fig.1), which is a PET imaging agent [9-11]. (*S,S*)-[^{11}C]MeNER **2** showed the highest hypothalamus to striatum (target to non-target) ratio of 2.5 at 60 min post-iv injection in rats. *In vitro* autoradiography of rat brain slices indicated that its localization correlated well with the known distribution of NET [9]. Imaging studies in nonhuman primates using (*S,S*)-[^{11}C]MeNER **2** exhibited a reasonable midbrain to striatum ratio of 1.4-1.6 [10]. One limitation was the longer time (60 min) required to obtain maximal specific binding due to slower clearance from the non-specific binding sites. The slower *in vivo* kinetics did not match the short half-life of carbon-11 (20 min) and diminished the clinical utility of this ligand. In comparison to (*S,S*)-[^{11}C]MeNER **2**, the corresponding (*R*)-[O-$^{11}CH_3$] -nisoxetine derivative **6** (Fig.1) exhibited very high non-specific binding *in vivo* [12,13]. None of the other ^{11}C labeled ligands for NET were as suitable as (*S,S*)-[^{11}C]MeNER **2** [14,15].

Due to the disadvantages of the ^{11}C labeled imaging agents described above, there is strong impetus to develop ^{18}F labeled probes for NET. ^{18}F-labelled fluoromethyl [(*S,S*)-[^{18}F] FMeNER] **3** (Fig.1) [16] as well as fluoroethyl [(*S,S*)[^{18}F]FRB] **4** (Fig.1) [17,18] derivatives of reboxetine have been reported. These ligands showed poor *in vivo* stability due to defluorination. Interestingly, deuterium substitution on the fluoroalkyl side-chain helped to reduce defluorination [16,17].

Extensive research has also been directed towards developing radiotracers for brain imaging of NET using SPECT [8,19,20]. In one of the initial efforts, we have found that ^{125}I-2-INXT **7**, (Fig.1) an iodinated nisoxetine derivative, displayed saturable binding with a high affinity (K_d = 0.06 nM) in the homogenates prepared from rat cortical tissues as well as homogenates prepared from cells over-expressing NET [8,23]. Biodistribution studies in rats showed a moderate target to non-target ratio (hypothalamus to striatum) of 1.5 at 3 hours post-iv. This was attributed to the higher non-specific binding of this ligand. Saji et al. evaluated the same compound (referred to as (*R*)-[^{125}I]MIPP) as a potential radiopharmaceutical for imaging cardiac [19] and brain NET [20] with SPECT and reported similar results.

Recently, a novel reboxetine derivative iodinated at position 2 of the phenoxy ring, (*S,S*)-IPBM **5** (also named as [^{123}I]INER) (Fig.1) has been reported [21,22]. (*S,S*)-IPBM **5** displayed high affinity and selectivity for NET in binding assay experiments. The (*S,S*) diastereomer (K_i = 4.22 nM) was found to be more potent than the racemic (K_i = 10.4 nM) and the (*R,R*) (K_i = 80.4 nM) diastereomer [21]. In biodistribution experiments, (*S,S*)-^{125}I-IPBM **5** provided a good initial uptake with maximum accumulation in the rat-brain at 30 minutes post–iv injection (0.54 % ID/gram at 30 min). The washout afterwards was relatively gradual. The regional cerebral distribution was consistent with the density of NET and a higher midbrain to striatum ratio was found at 180 minutes post injection [21]. A similar brain distribution pattern was observed in dynamic SPECT imaging of baboon using **5** [22]. Although the longer physical half-life of ^{123}I (13.3 h) is compatible with the slower kinetics of this ligand, it is still far from ideal as a specific brain imaging agent for NET. None of the above ligands fully meet the criteria for a good NET imaging agent.

In our attempts to develop optimal radiotracers for imaging NET, we have focused on the modification of the nisoxetine core structure. For example, we replaced one of the benzene rings of 2-INXT **7**, with a pyridine ring. This was expected to reduce the lipophilicity of [^{125}I] **7** without altering the binding affinity and selectivity for NET. In this paper, we are reporting the syntheses and initial screening of a novel series of pyridyl substituted nisoxetine derivatives, **8-11.** For the most promising compound, **9** (PYINXT), (*R*)-*N*-methyl-3-(3-iodopyridin-2-yloxy)-3-phenylpropylamine, we synthesized the corresponding radiolabeled [^{125}I]PYINXT. The results of biological evaluations have been encouraging, indicating that [^{125}I]PYINXT may be a useful candidate for mapping NET binding sites in the brain.

2. Results and Discussion

2.1 Chemistry

The synthesis of Compounds **8-11** is depicted in Scheme 1. The starting material (*S*)-(3-methylamino)-1-phenylpropan-1-ol **12**, was prepared according to a reported method [24]. Selective Boc-protection of the secondary amine led to the corresponding (*S*)-*tert*-butyl carbamate **13** in good yields. Compound **13** was used as a common intermediate in the synthesis of nisoxetine derivatives **8** and **10**. The coupling product **15** was obtained by the Mitsunobu reaction [25] of commercially available 3-bromo-2-hydroxypyridine **14** with **13**. Initial attempts to remove the Boc protecting group of **15** using TFA resulted in the cleavage of the pyridyl ether. Eventually, the deprotection was successfully carried out using trimethylsilyl trifluoromethanesulfonate (TMSOTf) and 2,6-lutidine in DCM at -40 °C [26] to provide Compound **8**. A very similar protocol was employed for the preparation of 4-iodo-3-hydroxy-pyridyl nisoxetine derivative **10** from the known 4-iodo-3-hydroxypyridine **17** [27].

Lithium-halogen exchange of the bromo-compound **15** with n-BuLi-iodine followed by deprotection using TMSOTf furnished the ‘cold’ iodinated derivative **9** (PYINXT). The corresponding debrominated side-product was also observed in the halogen exchange reaction. In addition to routine NMR analysis, the purity of Compound **9** was confirmed by HPLC (Phenonemex Gemini column, 4.6 × 25 cm; isocratic solvent: CH_3CN/ ammonium formate (1mM) = 9/1; flow rate: 0.5 ml/min, retention time 5.6 min).

A different approach was applied to the synthesis of Compound **11**. The key step involved the Mitsunobu reaction of commercially available (*S*)-3-chloro-1-phenylpropan-1-ol **19** with 2-iodo-3-hydroxypyridine **20** to derive Compound **21**. Substitution of chloride using aqueous methylamine afforded the expected product **11**. The hydrochloride salt was obtained by treating the free amine with 2N HCl in ethyl acetate.

Palladium catalyzed stannylation of Compound **8** using hexabutylditin and $Pd(PPh_3)_4$ furnished Compound **22** which was used as the radioiodination precursor for the synthesis of [^{125}I]PYINXT (Scheme 2). The radioiodinated ligand, [^{125}I]PYINXT was compared with the standard cold compound **9** showing an identical retention time of 5.6-5.8 min on HPLC (Phenonemex Gemini column, 4.6 × 25 cm; isocratic solvent: CH_3CN/1 mM ammonium formate = 9/1; flow rate: 0.5 ml/min). [^{125}I]PYINXT has been shown to be stable in 100% ethanol for up to two months after radioiodination (> 95% radiochemical purity determined by HPLC).

2.2 Biological evaluations

The cloned cell-line, LLC-PK_1, which over-expresses monoamine transporters, has been reported previously [28]. These cells are grown and maintained in our laboratory providing a convenient source of specific DAT, SERT or NET protein for *in vitro* binding assays. Because it is easy, readily available and provides comparable data for *in vitro* binding assays, our lab

has used the cells expressing the specific transporter instead of membrane homogenates of rat frontal cortex or striatum to screen monoamine transporter inhibitors [29]. The compounds **8-11** synthesized and reported in this paper were subjected to binding evaluations for the monoamine transporters NET, SERT and DAT. As expected, these nisoxetine derivatives showed very high selectivity for NET with more than 100 to 1000 fold less affinity for the other two monoamine transporters SERT and DAT (Table 1). Nisoxetine, a known selective ligand for NET, competes effectively with [^{125}I]2-INXT binding showing a K_i value of 4.8 ± 1.7 nM. Under similar assay conditions, the bromo derivative **8** and the iodo derivative PYINXT showed similar potency as nisoxetine with K_i values of 5.3 ± 0.3 and 4.5 ± 0.7 nM, respectively (Table 1). On the other hand, derivatives **10** and **11** had lower binding affinities with higher K_i values of 32.5 ± 5.5 and 13.5 ± 2.5 nM, respectively (Table 1). It is interesting to note that varying the position of nitrogen on the pyridine ring had a significant impact on binding affinity to NET. 2-Hydroxypyridine derivatives **8** and **9** (PYINXT) performed better than the 3-hydroxypyridine derivatives **10** and **11**. Based on the initial screening results, the radioiodinated derivative [^{125}I]PYINXT was prepared and subjected to further biological evaluation.

Specific binding of [^{125}I]PYINXT to NET was further examined using membrane homogenates prepared from LLC-NET cells. Scatchard transformation of the saturation binding data gave a linear plot indicating one-site binding (data not shown). The mean values from 3 experiments gave a K_d value of 0.53± 0.05 nM, which is higher than the value obtained with the previous ligand [^{125}I]2-INXT (K_d = 0.06 ± 0.01 nM) [8]. It is important to note that the K_i and the K_d values for **9** are different. The ten-fold difference between K_i and K_d is most likely due to the very high binding affinity of [^{125}I]2-INXT (K_d = 0.06 nM in LLC-NET) used in the assay for K_i estimation.

The biodistribution of [^{125}I]PYINXT in different organs and brain regions after an i.v. injection is shown in Table 2. The initial brain uptake at 2 minutes post-injection was moderate (0.54 %dose/organ) indicating a less efficient passage of the tracer through the intact blood-brain barrier. Radioactivity levels in all brain regions were the highest at 2 minutes and then gradually decreased over the 4 hour period. The washout rate was faster in striatum, where no NET binding sites are located, as compared to other brain regions (i.e. cerebellum, hippocampus, cortex and hypothalamus where different levels of NET are concentrated). At 240 minutes postinjection, regions containing norepinephrine innervation showed higher concentrations of radioactivity than the striatum (0.04, 0.04, 0.03, 0.06 and 0.03 % dose/gram for cerebellum, hippocampus, cortex, hypothalamus and striatum respectively). The ratio of hypothalamus to striatum, representing the target to non-target ratio, was about 2.1 (Table 2). This value is slightly higher than the ratio reported previously for [^{125}I]INXT **7** [8] and it is comparable to the ratio reported for ^{11}C-MeNER, **2**, a reboxetine derivative [9]. Despite the lower *in vitro* binding affinity of [^{125}I]PYINXT for NET (K_d = 0.53 nM in LLC-NET) as compared to [^{125}I]INXT **7** (K_d = 0.06 nM in LLC-NET), it displayed more favorable *in vivo* kinetic properties (relative fast washout thus resulting in a slightly higher target (HY) vs. non-target (ST) ratio) (Table 2). As expected, the lipophilicity of [^{125}I]PYINXT, because of the substitution of the phenyl ring with the pyridine ring, is lower than that of [^{125}I]INXT **7** (log P = 1.45 for [^{125}I]PYINXT and logP = 1.96 for [^{125}I]INXT **7**). This combination of lower lipophilicity together with the good selectivity and specific binding affinity of [^{125}I]PYINXT for NET appears to account for the *in vivo* target vs non-target signal. The new NET probe [^{125}I]PYINXT, reported here meets a majority of the criteria for an ideal NET imaging agent, i.e. a high binding affinity; a high selectivity (>100 fold); easily labeled and a ratio of target vs. non-target >2. The moderate initial brain uptake of [^{125}I]PYINXT **(**0.54 %dose/organ at 2 min) is consistent with the values reported for other NET imaging agents in rats ([^{125}I]INXT **7** = 0.56 at 2 min) [8]; ((*S*,*S*)-[^{11}C]MeNER **2** = 0.53 at 5 min) [9]; ((*S*,*S*)-^{125}I-IPBM **5** = 0.89 at 5 min) [21]. This general phenomenon, which is independent of the lipophilicity of the

ligands, might be an inherent property of the common backbone structure for diffusion across the intact blood-brain barrier. This may be a limitation for the development of ideal imaging agents based on nisoxetine or reboxetine structures. Also noteworthy is the striking difference between the brain uptake in rats and mice. In mice, [^{125}I]PYINXT showed a higher initial uptake (1.23 % dose/organ at 2 min post injection; data not shown) compared to the uptake in rats (0.54 % dose/organ at 2 min post injection). Saji et al. reported a very similar observation in the case of [^{125}I]INXT **7** (0.97 % dose/organ at 2 min post injection in mice and 0.45 % dose/organ at 5 min post injection in rats) [20]. We have no simple explanation for this observation. However, it seems that in developing probes for NET, species differences may require careful evaluation.

At 120 min post-injection of [^{125}I]PYINXT, autoradiograms of rat brain sections showed an intense labeling in several regions [30], i.e. locus coerulus, thalamic and hypothalamic nuclei and bed nucleus of the strai terminalis (Fig.2, top row), areas known to have high densities of NET sites [31]. A medium level of labeling was observed in the median raphe, and dentate gyrus. Lower, but detectable labeling was also found in the frontal cortex. The caudate putamen showed the lowest labeling. The regional distribution observed with [^{125}I]PYINXT is consistent with that reported for other NET ligands [32-34] indicating that the *in vivo* binding of [^{125}I]PYINXT in rat brain strongly correlates with known NET density distribution in different brain regions. Nisoxetine pretreatment completely abolished the labeling for NET (shown in Fig.2, bottom row) indicating that [^{125}I]PYINXT and nisoxetine compete for the same binding site (NET) *in vivo*.

The development of an ideal imaging agent for NET is challenging due to the very low density of NET binding sites in the brain. Previous estimations in our laboratory have shown that the B_{max} of NET is significantly lower than that of SERT and DAT (55 fmol/mg protein, 194 fmol/mg protein and 2000 fmol/mg protein for NET, SERT and DAT respectively) [8]. Hence, an important prerequisite for a useful NET tracer is that it should display very high binding affinity and selectivity. Despite the high binding affinity and selectivity *in vitro*, iodinated ligands reported so far such as [^{125}I]INXT **7** and (*S,S*)-^{125}I-IPBM **5**, displayed rather slower *in vivo* kinetics. For [^{125}I]INXT **7** higher non-specific binding was observed. Assuming that the non-specific binding could be minimized by adjusting the lipophilicity of the molecule, we synthesized a new pyridyl substituted nisoxetine derivative [^{125}I]PYINXT. It was successfully characterized *in vitro* and *in vivo* as targeting NET. The binding affinity of [^{125}I]PYINXT to NET was lower than that of [^{125}I]INXT **7**, but [^{125}I]PYINXT exhibited comparable initial uptake, improved kinetics and specific binding in the rat brain. Furthermore, the in vivo stability of [^{125}I]PYINXT to be qualified as a suitable platform structure remains to be determined. The new ligand, [125I]PYINXT is not yet ideal, but undoubtedly, it represents progress in the quest for better imaging agents for NET using SPECT. In addition, it may be interesting to evaluate the potential of [^{125}I]PYINXT for imaging cardiac sympathetic innervation. Presently, we are also working on the extension of the same strategy to develop suitable pyridyl-reboxetine analogues targeting NET.

In conclusion, in a search for potential SPECT imaging agents for NET, a new series of nisoxetine derivatives was developed by replacing one of the phenyl rings with a pyridine ring. These novel nisoxetine derivatives displayed good binding affinities to NET (K_i values between 5 and 30 nM). The radioiodinated probe [^{125}I]PYINXT displayed a high and selective binding to NET in the rat brain. Further evaluation of this ligand and its congeners may lead to useful imaging agents for mapping NET sites in the living human brain.

3. Materials and methods

3.1 General

All reagents used in the synthesis were commercial products and were used without purification, unless otherwise indicated. ^{1}H and ^{13}C nuclear magnetic resonance (NMR) spectra were obtained with a Bruker DPX 200 spectrometer for all compounds except **21** and **11** (DPX 400). Chemical shifts are reported as δ values with respect to residual $CHCl_3$ proton in $CDCl_3$ for ^{1}H NMR and residual $CHCl_3$ carbons in $CDCl_3$ for ^{13}C NMR, unless otherwise mentioned. Coupling constants are reported in Hertz. Multiplicities are defined as: s (singlet), d (doublet), dd (doublet of doublet), t (triplet), br (broad), m (multiplet). Preparative thin layer chromatography (PTLC) was performed with Analtech Uniplate (20 × 20; 2000 μm). Chromatography refers to flash chromatography on silica gel, unless otherwise indicated. Electrospray ionization mass spectra were recorded with LC MSD TOF, Agilent Technologies. High resolution mass spectra for compounds **21** and **11** were obtained with JMS-HX110/110 Tandem Mass Spectrometer, JEOL Ltd. Optical rotations were measured with a Perkin Elmer 243B polarimeter. [^{125}I]NaI (0.1 N NaOH solution) was purchased from DuPont NEN Research (Boston, MA).

3.1.1 (S)-tert-butyl-3-hydroxy-3-phenylpropyl(methyl)carbamate (13)—A solution of (*S*)-3-(methylamino)-1-phenylpropan-1-ol (**12**) (1.27 g, 7.6 mmol) in DCM (20 mL) was stirred at room temperature. 4N NaOH (337 mg, 8.4 mmol) was added to this dropwise. After 5 minutes Boc-anhydride (1.67 g, 7.6 mmol) was added and the reaction mixture stirred for 4 h. Water (20 mL) was added and the mixture was extracted with DCM (3 × 50 mL). The combined organic layers were washed with brine, dried over anhydrous sodium sulfate and the solvent evaporated. The residue was purified by chromatography (75:25 hexane-ethyl acetate) to give Compound **13** (1.2 g, 59 %). $[\alpha]_D^{20} = -5.7$ (c = 0.94, $CHCl_3$). ^{1}H NMR (200 MHz, $CDCl_3$): δ 7.35-7.23 (m, 5H), 4.59 (d, *J* = 7.7 Hz, 1H), 3.86 (br, 1H), 3.08 (br, 1H), 2.86 (s, 3H), 2.02-1.86 (m, 2H), 1.46 (s, 9H).

3.1.2 (R)-tert-butyl-3-(3-bromopyridin-2-yloxy)-3-phenylpropyl(methyl) carbamate (15)—Under inert atmosphere, 3-Bromo-2-hydroxypyridine (**14**) (489 mg, 2.81 mmol) was added to a solution of Compound **13** (572 mg, 2.16 mmol) and Pph_3 (848 mg, 3.24 mmol) in diethylether (15 mL). The resulting suspension was stirred at 0 °C for 10 minutes followed by the dropwise addition of DIAD (0.63 mL, 3.24 mmol) over 5 minutes. The reaction mixture was warmed to room temperature and stirred for 3 h. The solvent was evaporated and the residue was adsorbed on silica gel. Purification by chromatography (75:25 hexane-ethyl acetate) afforded the product **15** (535 mg, 58 %). $[\alpha]_D^{20} = -25.0$ (c = 1.3, $CHCl_3$). ^{1}H NMR (200 MHz, $CDCl_3$): δ 7.92 (d, *J* = 4.8 Hz, 1H), 7.71 (d, *J* = 7.6 Hz, 1H), 7.43-7.20 (m, 5H), 6.66-6.60 (m, 1H), 6.15 (dd, *J* = 4.8 Hz, 7.8 Hz, 1H), 3.50-3.36 (m, 2H), 2.82 (s, 3H), 2.34-2.04 (m, 2H), 1.37 (s, 9H).

3.1.3 (R)-N-methyl-3-(3-bromopyridin-2-yloxy)-3-phenylpropan-1-amine (8)—A solution of the Boc-protected compound **15** (263 mg, 0.62 mmol) and 2,6- lutidine (401 mg, 3.75 mmol) in DCM (7 mL) was stirred at -40 °C for 10 minutes under inert atmosphere. Trimethylsilyl trifluoromethanesulfonate (555 mg, 2.5 mmol) was carefully added to this dropwise. The reaction mixture was allowed to warm to room temperature over 2 h. After the addition of aqueous Na_2CO_3 (10 %, 10 mL), the reaction mixture was extracted with DCM (3 × 20 mL). The organic phase was washed with brine, dried over anhydrous Na_2SO_4 and the solvent removed under reduced pressure. The pure product **8** (165 mg) was isolated from the residue by gradient chromatography (8:2 hexane-ethylacetate to 9:1:1 DCM-MeOH-triethylamine) in 82 % yield. $[\alpha]_D^{20} = -25.1$ (c = 0.95, $CHCl_3$). ^{1}H NMR (200 MHz, $CDCl_3$):

δ 7.97 (dd, J = 1.6 Hz, 4.8 Hz, 1H), 7.76 (dd, J = 1.6 Hz, 7.6 Hz, 1H), 7.53-7.18 (m, 5H), 6.70 (dd, J = 4.8 Hz, 7.6 Hz, 1H), 6.28-6.22 (m, 1H), 5.28 (br, 1H), 2.84 (t, J = 7.1 Hz, 2H), 2.49 (s, 3H), 2.39-2.24 (m, 2H). ^{13}C NMR (50 MHz, $CDCl_3$): δ 158.57, 145.09, 141.41, 140.48, 128.05, 127.24, 125.69, 117.68, 107.10, 75.45, 46.99, 35.42, 34.74. HRMS (ESI) calcd for $C_{15}H_{18}BrN_2O$ $[M + H]^+$ 321.0603, found 321.0605.

3.1.4 (R)-tert-butyl-3-(3-iodopyridin-2-yloxy)-3-phenylpropyl(methyl)carbamate (16)—To a solution of the bromo-compound **15** (142 mg, 0.33 mmol) and TMEDA (78 μL, 0.53 mmol) in anhydrous THF (3 mL) stirred at -78 °C under inert atmosphere, n-BuLi (1.6 M in hexanes, 281 μL, 0.44 mmol) was added dropwise. The reaction mixture was stirred at -78 °C for 1 h before the addition of iodine (133 mg, 0.53 mmol) in THF (2 mL). After stirring for another hour at -78 °C, the reaction mixture was warmed to room temperature and stirred for an additional 15 minutes. Saturated aqueous NH_4Cl (5 mL) was added and the resulting mixture extracted with DCM (3 × 15 mL). The organic phase was washed with brine, dried over anhydrous Na_2SO_4 and the solvent removed under reduced pressure. The crude reaction mixture was purified by careful chromatography (9:1 hexane-ethyl acetate) to afford **16** as colorless oil (46 mg, 30 % yield). The debrominated side product was also isolated (25 mg, 22 %). $[\alpha]_D^{20} = -45.8$ (c = 1.36, $CHCl_3$). ^{1}H NMR (200 MHz, $CDCl_3$): δ 8.00–7.96 (m, 2H), 7.44-7.18 (m, 5H), 6.56 (dd, J = 5.3 Hz, 7.0 Hz, 1H), 6.11 (dd, J = 4.8 Hz, 7.9 Hz, 1H), 3.50-3.36 (m, 2H), 2.83 (s, 3H), 2.22-2.07 (m, 2H), 1.37 (s, 9H).

3.1.5 (R)-N-methyl-3-(3-iodopyridin-2-yloxy)-3-phenylpropan-1-amine (9)—The procedure described before for the deprotection of Compound **15** was applied to Compound **16** (45 mg, 0.096 mmol). The reaction mixture was purified by PTLC (9:1:1 DCM-MeOH-triethylamine) to obtain the title Compound **9** (25 mg, 71 %) as colorless oil. $[\alpha]_D^{20} = -38.0$ (c = 0.72, $CHCl_3$). ^{1}H NMR (200 MHz, $CDCl_3$): δ 8.02–7.99 (m, 2H), 7.44-7.20 (m, 5H), 6.64-6.58 (m, 1H), 6.27-6.21 (m, 1H), 3.06-2.99 (m, 2H), 2.57 (s, 3H), 2.47 (br, 2H). ^{13}C NMR (50 MHz, $CDCl_3$): δ 160.21, 147.97, 146.10, 139.61, 127.95, 127.09, 125.65, 117.94, 80.13, 75.30, 46.09, 33.68, 33.33 HRMS (ESI) calcd for $C_{15}H_{18}IN_2O$ $[M + H]^+$: 369.0464, found 369.0421.

3.1.6 (R)-tert-butyl-3-(4-iodopyridin-3-yloxy)-3-phenylpropyl(methyl)carbamate (18)—Mitsunobu reaction of 4-iodo-3-hydroxypyridine **17** (183 mg, 1.05 mmol) with Compound **13** (215 mg, 0.81 mmol) was carried out as described for the preparation of Compound **15**. The reaction mixture was purified by chromatography (7:3 hexane-ethyl acetate) to provide the product **18** (151 mg, 39 %). $[\alpha]_D^{20} = -63.4$ (c = 1.48, $CHCl_3$). ^{1}H NMR (200 MHz, $CDCl_3$): δ 7.83 (s, 1H), 7.75 (d, J = 4.8 Hz, 1H), 7.67 (d, J = 4.8 Hz, 1H), 7.33-7.26 (m, 5H), 5.28 (dd, J = 4.1 Hz, 8.3 Hz, 1H), 3.53-3.45 (m, 2H), 2.86 (s, 3H), 2.35-2.03 (m, 2H), 1.37 (s, 9H).

3.1.7 (R)-N-methyl-3-(4-iodopyridin-3-yloxy)-3-phenylpropan-1-amine (10)—The procedure described before for the deprotection of Compound **15** was applied to Compound **18** (99 mg, 0.21 mmol). The reaction mixture was purified by PTLC (95:5:0.5 DCM-MeOH-NH_4OH) to afford the title Compound **10** (35 mg, 45 %). $[\alpha]_D^{20} = -59.4$ (c = 1.35, $CHCl_3$). ^{1}H NMR (200 MHz, $CDCl_3$): δ 7.87 (s, 1H), 7.74 (d, J = 4.9 Hz, 1H), 7.66 (d, J = 4.9 Hz, 1H), 7.34-7.25 (m, 5H), 5.45 (dd, J = 4.7 Hz, 8.0 Hz, 1H), 3.60 (br, 1H), 2.94-2.77 (m, 2H), 2.47 (s, 3H), 2.42-2.05 (m, 2H). ^{13}C NMR (50 MHz, $CDCl_3$): δ 152.78, 142.69, 138.59, 135.53, 133.81, 128.70, 128.15, 125.56, 97.81, 79.10, 46.60, 36.11, 34.07. HRMS (ESI) calcd for $C_{15}H_{18}IN_2O$ $[M + H]^+$: 369.0464, found 369.0443.

3.1.8 (R)-3-(3-chloro-1-phenylpropoxy)-2-iodopyridine (21)—A solution of (*S*)-3-chloro-1-phenylpropan-1-ol **19** (340 mg, 2 mmol) and PPh_3 (530 mg, 2.02 mmol) in anhydrous THF (2 mL) was cooled to 0 °C. 2-iodo-3-hydroxypyridine (442 mg, 2 mmol) was added to the reaction mixture and it was stirred at 0 °C for 5 min before the dropwise addition of DIAD (424 mg, 2.1 mmol) over another 5 min. After 30 minutes, the solvent was evaporated and the residue dissolved in DCM and purified by flash chromatography (4:1 hexane-ethyl acetate) to provide **21** (485 mg, 65 %) as a clear oil. ^{1}H NMR (400 MHz, $CDCl_3$): δ 7.91 (m, 1H), 7.42-7.34 (m, 5H), 7.28 (m, 2H), 5.72 (m, 1H), 3.83 (m, 1H), 3.64 (m, 1H), 2.62 (m, 1H), 2.38 (m, 1H).

3.1.9 (R)-N-methyl-3-(2-iodopyridin-3-yloxy)-3-phenylpropan-1-amine (11)—A solution of **21** (190 mg, 0.5 mmol) and methyl amine (2 mL, 40 % wt. in water) in ethanol (2 mL) was heated in a sealed flask at 80 °C for 2 h. The solvent was removed and the residue purified by flash chromatography (5:1 ethyl acetate-methanol) to provide **11** (126 mg, 67 %) as a clear oil. The free amine was dried under vacuum for 2 days and stored in the freezer. ^{1}H NMR (400 MHz, CD_3OD): δ 7.90 (d, J = 3.2 Hz, 1H), 7.38 (m, 5H), 6.99 (dd, J = 1.6 Hz, 3.2 Hz 1H), 6.86 (dd, J = 1.6 Hz, 3.2 Hz, 2H), 5.63 (m, 1H), 3.34 (m, 1H), 3.20 (m, 1H), 2.78 (m, 2H). 2.74 (s, 3H). HRMS (FAB^+) calcd for $C_{15}H_{18}IN_2O$ $[M + H]^+$: 369.0464, found 369.0453.

3.2.0 (R)-N-methyl-3-[3-(tributylstannyl)pyridin-2-yloxy]-3-phenylpropan-1-amine (22)—A suspension of bromo-compound **8** (89 mg, 0.28 mmol) and $Pd(PPh_3)_4$ (33 mg, 0.028 mmol) in hexabutylditin (0.75 mL, 1.4 mmol) was refluxed at 110 °C for 6 h. After cooling to room temperature, the reaction mixture was treated with aqueous KF solution (10 %, 10 mL) followed by aqueous Na_2CO_3 solution (10 %, 10 mL). It was extracted with DCM-MeOH (95:5) mixtures (5 × 15 mL). The organic phase was washed with brine, dried over anhydrous Na_2SO_4 and the solvent removed under reduced pressure. The crude residue was purified by PTLC (9:1 DCM-MeOH) to give the expected product **22** , *albeit* in low yield (19 mg, 13 %). ^{1}H NMR (200 MHz, $CDCl_3$): δ 8.01 (dd, J = 1.9 Hz, 4.9 Hz, 1H), 7.63 (dd, J = 2.0 Hz, 6.8 Hz, 1H), 7.42-7.23 (m, 5H), 6.81-6.79 (m, 1H), 6.19 (t, J = 6.8 Hz, 1H), 3.81 (br, 1H), 2.84-2.62 (m, 2H), 2.49 (s, 3H), 2.34-2.16 (m, 2H), 1.60-1.21 (m, 15H), 1.07-0.82 (m, 12H).

3.2 Preparation of [125I]PYINXT

Preparation of the radioiodinated tracer, [125I]PYINXT was carried out by an iododestannylation reaction from the corresponding tin precursor catalyzed by hydrogen peroxide as described previously [35]. The no-carrier-added product [125I]PYINXT with a high specific activity (2,200 Ci/mmol) was obtained via a simple C4 mini-column. In brief, after quenching with sodium bisulfite and neutralizing with sodium bicarbonate, the reaction mixture was loaded on a reversed phase C4 mini-column (Vydac BioSelect, CA, 1 × 6 cm). After washing the column with 3 ml of 10% EtOH, the desired product [125I]PYINXT was then eluted with 0.5 ml of ethanol. The radiochemical purity of the ligand was examined on HPLC using a reversed-phase column (Phenomenex Gemini C18 analytical column, 4.6 × 250 mm, 5 μm, CH_3CN/Ammonium formate buffer (1 mM) 9/1; flow rate 0.5 mL/min).

3.3 In vitro binding assays

[^{125}I]2-INXT [8], [^{125}I]IDAM [36] and [^{125}I]IPT [37] were prepared according to the procedures described previously. Nisoxetine, Citalopram and GBR12909 were obtained from Sigma Biochemical Inc. LLC-PK_1 cells over-expressing three monoamine transporters, named respectively as norepinephrine transporters (LLC-NET), serotonin transporters (LLC-SERT) and dopamine transporters (LLC-DAT), were kindly provided by Dr. G. Rudnick of Yale University. Cells were plated and grown to confluence as a monolayer as described before [28]. The membrane homogenates were prepared and used for the binding assays with the known characterized radioiodinated ligands [^{125}I]2-INXT for NET, [^{125}I]IDAM for SERT and [^{125}I]IPT for DAT. Binding assays were performed in glass tubes (12 × 75 mm) with a final

volume of 0.5 ml. In saturation experiments, aliquots (100 μl corresponding to 40-60 μg of protein) of membrane suspensions were mixed with buffer (50 mM Tris-HCl, pH 7.4, 120 mM NaCl, 5 mM KCl) containing 0.05-2.0 nM [125I]PYINXT. Competition experiments were performed using 0.05-0.06 nM [^{125}I]2-INXT for NET, 0.1 nM [^{125}I]IDAM for SERT and 0.2 nM [^{125}I]IPT for DAT and 8-10 concentrations (10^{-10}-10^{-5}M) of competing drugs. Inhibitors were serially diluted with the buffer (as above) containing 0.1% BSA to overcome the stickiness and loss due to dilution. Nonspecific binding was defined with 1 μM nisoxetine (for NET) or 1 μM citalopram (for SERT) or 1 μM GBR12909 (for DAT). Incubation was carried out for 60 min at room temperature and then terminated by separation of bound from free radioligand by filtration through glass fiber filters (Schleicher & Schuell No. 25, Keene, NH) presoaked with 1% polyethylenimine. The filters were then washed three times with 3 ml of ice-cold 20 mM Tris buffer and counted in a gamma counter (Cobra II, Perkin Elmer) with 70 % efficiency. The results of saturation and competition experiments were subjected to nonlinear regression analysis using EBDA [38] to obtain K_d and K_i values.

3.4 Biodistribution in rats

Male Sprague-Dawley rats weighing 225-275 g were used in the studies. Three rats per group were used for biodistribution study. While under isoflurane anesthesia, 0.2 ml of a saline solution containing 10 μCi of radioactive tracer was injected into the femoral vein. The rats were sacrificed at the time indicated by cardiac excision while under anesthesia. Organs of interest were removed and weighed, and the radioactivity was counted. The percent dose per organ was calculated by a comparison of the tissue counts to counts of 1% of the initial dose (100 times diluted aliquots of the injected material) measured at the same time. Regional brain distribution in rats was measured after an i.v. injection of the radioactive tracer. Samples from different brain regions [cortex (CX), striatum (ST), hippocampus (HP), cerebellum (CB) and hypothalamus (HY)] were dissected, weighed and counted. The percentage dose/g of each sample was calculated by comparing sample counts with the counts of the diluted initial dose described above. The striatum region containing no NET was used as a background region and ratios of target to background region were obtained.

3.5 Ex vivo autoradiography of [^{125}I]PYINXT in rat brain

Rats under isoflurane anesthesia were injected intravenously with 0.3 ml of a saline solution containing 300 μCi of [^{125}I]PYINXT. At 120 min post i.v. injection, the animals were sacrificed by cardiac excision while under isoflurane anesthesia. The brains were rapidly removed, placed in embedding medium (Tissue Tek, Miles Laboratory, Elkhart, IN) and frozen with powdered dry ice. After reaching equilibrium at -20 °C, consecutive 20 μm coronal sections were cut on a cryostat microtome (Hacker Instruments, Fairfield, NJ), thaw-mounted on microscope slides, and air-dried at room temperature. The slides containing the brain sections were exposed to Kodak Biomax MR film along with 20 μm thick ^{125}I standards (Amersham Corp., Arlington, Ill) for three days in autoradiographic cassettes. A second group of rats was pretreated with nisoxetine (10 mg/kg, i.v. 10 min prior to [^{125}I]PYINXT) and then injected with [^{125}I]PYINXT and given the same treatment described above. The *ex vivo* autoradiograms of nisoxetine-treated brains were compared to the untreated control brains for NET labeling.

3.6 Partition coefficient

Partition coefficients were measured by mixing the [^{125}I]PYINXT with 3g each of 1-octanol and buffer (0.1 M phosphate, pH 7.4) in a test tube. The test tube was vortexed for 3 min at room temperature, followed by centrifugation for 5 min. Two weighed samples (0.5 g each) from the 1-octanol and buffer layers were counted in a well counter. The partition coefficient was determined by calculating the ratio of cpm/g of 1-octanol to that of buffer. Samples from

the 1-octanol layer were re-partitioned until consistent partitions of coefficient values were obtained. The measurement was done in triplicate and repeated three times.

Acknowledgements

The work was supported by the grants awarded from the National Institute of Health (NS5049438 to H.F. Kung) and (R21 MH074008-01A1 to R. Waterhouse).

References

1. Amara SG, Kuhar MJ. Neurotransmitter transporters: recent progress. Annu Rev Neurosci 1993;16:73–93. [PubMed: 8096377]
2. Blakely RD, Bauman AL. Biogenic amine transporters: regulation in flux. Current Opinion in Neurobiology 2000;10:328–336. [PubMed: 10851182]
3. Zhu M-Y, Ordway GA. Down-regulation of norepinephrine transporters on PC12 cells by transporter inhibitors. J Neurochem 1997;68:134–41. [PubMed: 8978719]
4. Klimek V, Stockmeier C, Overholser J, Meltzer HY, Kalka S, Dilley G, Ordway GA. Reduced Levels of Norepinephrine Transporters in the Locus Coeruleus in Major Depression. J Neurosci 1997;17:8451–58. [PubMed: 9334417]
5. Biederman J, Spencer T. Attention-deficit/hyperactivity disorder (ADHD) as a noradrenergic disorder. Biol Psychiatry FIELD Full Journal Title:Biological psychiatry 1999;46:1234–42.
6. Viggiano D, Ruocco LA, Arcieri S, Sadile AG. Involvement of norepinephrine in the control of activity and attentive processes in animal models of Attention Deficit Hyperactivity Disorder. Neural Plas 2004;11:133–49.
7. Tejani-Butt SM, Yang J, Zaffar H. Norepinephrine transporter sites are decreased in the locus coeruleus in Alzheimer's disease. Brain Res FIELD Full Journal Title:Brain research 1993;631:147–50.
8. Kung MP, Choi SR, Hou C, Zhuang ZP, Foulon C, Kung HF. Selective binding of 2-[125I]iodo-nisoxetine to norepinephrine transporters in the brain. Nucl Med Biol 2004;31:533–41. [PubMed: 15219270]
9. Wilson AA, Patrick Johnson D, Mozley D, Hussey D, Ginovart N, Nobrega J, Garcia A, Meyer J, Houle S. Synthesis and in vivo evaluation of novel radiotracers for the in vivo imaging of the norepinephrine transporter. Nucl Med Biol 2003;30:85–92. [PubMed: 12623106]
10. Schou M, Halldin C, Sovago J, Pike VW, Gulyas B, Mozley PD, Johnson DP, Hall H, Innis RB, Farde L. Specific in vivo binding to the norepinephrine transporter demonstrated with the PET radioligand, (S,S)-[(11)C]MeNER. Nucl Med Biol 2003;30:707–14. [PubMed: 14499328]
11. Ding YS, Lin KS, Garza V, Carter P, Alexoff D, Logan J, Shea C, Xu Y, King P. Evaluation of a new norepinephrine transporter PET ligand in baboons, both in brain and peripheral organs. Synapse 2003;50:345–52. [PubMed: 14556239]
12. Haka M, Kilbourn M. Synthesis and regional mouse brain distribution of [11C]-nisoxetine, a norepinephrine uptake inhibitor. Nucl Med Biol 1989;16:771–74.
13. Ding Y-S, Lin K-S, Logan J, Benveniste H, Carter P. Comparative evaluation of positron emission tomography radiotracers for imaging the norepinephrine transporter: (S,S) and (R,R) enantiomers of reboxetine analogs ([11C]methylreboxetine, 3-Cl-[11C]methylreboxetine and [18F] fluororeboxetine), (R)-[11C]nisoxetine, [11C]oxaprotiline and [11C]lortalamine. J Neurochem 2005;94:337–51. [PubMed: 15998285]
14. Schou M, Pike VW, Varrone A, Gulyas B, Farde L, Halldin C. Synthesis and PET evaluation of (R)-[S-methyl-11C]thionisoxetine, a candidate radioligand for imaging brain norepinephrine transporters. J Lab Compds Radiopharm 2006;49:1007–19.
15. Schou M, Pike VW, Sovago J, Gulyas B, Gallagher PT, Dobson DR, Walter MW, Rudyk H, Farde L, Halldin C. Synthesis of 11C-labelled (R)-OHDMI and CFMME and their evaluation as candidate radioligands for imaging central norepinephrine transporters with PET. Bioorg Med Chem 2007;15:616–25. [PubMed: 17123820]
16. Schou M, Halldin C, Sovago J, Pike VW, Hall H, Gulyas B, Mozley PD, Dobson D, Shchukin E, Innis RB, Farde L. PET evaluation of novel radiofluorinated reboxetine analogs as norepinephrine transporter probes in the monkey brain. Synapse 2004;53:57–67. [PubMed: 15170818]

17. Lin KS, Ding YS, Kim SW, Kil KE. Synthesis, enantiomeric resolution, F-18 labeling and biodistribution of reboxetine analogs: promising radioligands for imaging the norepinephrine transporter with positron emission tomography. Nucl Med Biol 2005;32:415–22. [PubMed: 15878511]

18. Ding Y-S, Lin K-S, Logan J. PET imaging of norepinephrine transporters. Curr Pharm Des 2006;12:3831–45. [PubMed: 17073682]

19. Kiyono Y, Kanegawa N, Kawashima H, Fujiwara H, Iida Y, Nishimura H, Saji H. A new norepinephrine transporter imaging agent for cardiac sympathetic nervous function imaging: radioiodinated (R)-N-methyl-3-(2-iodophenoxy)-3-phenylpropanamine. Nucl Med Biol 2003;30:697–706. [PubMed: 14499327]

20. Kiyono Y, Kanegawa N, Kawashima H, Kitamura Y, Iida Y, Saji H. Evaluation of radioiodinated (R)-N-methyl-3-(2-iodophenoxy)-3-phenylpropanamine as a ligand for brain norepinephrine transporter imaging. Nucl Med Biol 2004;31:147–53. [PubMed: 15013479]

21. Kanegawa N, Kiyono Y, Kimura H, Sugita T, Kajiyama S, Kawashima H, Ueda M, Kuge Y, Saji H. Synthesis and evaluation of radioiodinated (S,S)-2-(alpha-(2-iodophenoxy)benzyl)morpholine for imaging brain norepinephrine transporter. Eur J Nucl Med Mol Imaging 2006;33:639–47. [PubMed: 16523308]

22. Tamagnan GD, Brenner E, Alagille D, Staley JK, Haile C, Koren A, Early M, Baldwin RM, Tarazi FI, Baldessarini RJ, Jarkas N, Goodman MM, Seibyl JP. Development of SPECT imaging agents for the norepinephrine transporters: [123I]INER. Bioorg Med Chem Lett 2007;17:533–37. [PubMed: 17095215]

23. Chumpradit S, Kung M-P, Panyachotipun C, Prapansiri V, Foulon C, Brooks BP, Szabo SA, Tejani-Butt S, Frazer A, Kung HF. Iodinated tomoxetine derivatives as selective ligands for serotonin and norepinephrine uptake sites. J Med Chem 1992;35:4492–97. [PubMed: 1447750]

24. Robertson DW, Krushinski JH, Fuller RW, Leander JD. Absolute configurations and pharmacological activities of the optical isomers of fluoxetine, a selective setotonin-uptake inhibitor. J Med Chem 1988:1412–17. [PubMed: 3260286]

25. Mitsunobu O. The use of diethyl azodicarboxylate and triphenylphosphine in synthesis and transformation of natural products. Synthesis 1981:1–25.

26. Bastiaans HMM, van der Baan JL, Ottenheijm HCJ. Flexible and Convergent Total Synthesis of Cyclotheonamide B. J Org Chem 1997;62:3880–89.

27. Lindstroem S, Ripa L, Hallberg A. Synthesis of Two Conformationally Constrained Analogues of the Minor Tobacco Alkaloid Anabasine. Org Lett 2000;2:2291–93. [PubMed: 10930266]

28. Gu H, Wall SC, Rudnick G. Stable expression of biogenic amine transporters reveals differences in inhibitor sensitivity, kinetics, and ion dependence. J Biol Chem 1994;269:7124–30. [PubMed: 8125921]

29. Oya S, Choi SR, Kung MP, Kung HF. 5-Chloro-2-(2'-((dimethylamino)methyl)-4'-iodophenylthio) benzenamine: a new serotonin transporter ligand. Nucl Med Biol 2007;34:129–39. [PubMed: 17307121]

30. Paxinos, G.; Watson, C. The Rat Brain In Stereotaxic Coordinates. New York: Academic Press; 1986.

31. Cortes R, Soriano E, Pazos A, Probst A, Palacios JM. Autoradiography of antidepressant binding sites in the human brain: localization using [3H]paroxetine. Nueroscience 1988;27:473–96.

32. De Souza EB, Kuyatt BL. Autoradiographic localization of 3H-paroxetine-labeled serotonin uptake sites in rat brain. Synapse 1987;1:488–96. [PubMed: 2975068]

33. Kovachich GB, Aronson CE, Brunswick DJ, Frazer A. Quantitative autoradiography of serotonin uptake sites in rat brain using [3H]cyanoimipramine. Brain Res 1988;454:78–88. [PubMed: 2970277]

34. Biegon A, Mathis CA, Hanrahan SM, Jagust WJ. [125I]5-Iodo-6-nitroquipazine: a potent and selective ligand for the 5-hydroxytryptamine uptake complex II in vivo studies in rats. Brain Res 1993;619:236–46. [PubMed: 8374782]

35. Kung MP, Hou C, Zhuang Z-P, Zhang B, Skovronsky DM, Gur T, Lee VM-Y, Trojanowski JQ, Kung HF. IMPY:An improved thioflavin-T derivative for in vivo Labeling of b-amyloid plaques. Brain Res 2002;956:202–10. [PubMed: 12445687]

36. Kung MP, Hou C, Oya S, Mu M, Acton PD, Kung HF. Characterization of [123I]IDAM as a novel single-photon emission tomography tracer for serotonin transporters. Eur J Nucl Med 1999;26:844–53. [PubMed: 10436197]

37. Kung M-P, Essman WD, Frederick D, Meegalla S, Goodman M, Mu M, Lucki I, Kung HF. IPT: a novel iodinated ligand for the CNS dopamine transporter. Synapse 1995;20:316–24. [PubMed: 7482291]

38. Munson PJ, Rodbard D. LIGAND: a versatile computerized approach for characterization of ligand-binding systems. Anal Biochem 1980;107:220–39. [PubMed: 6254391]

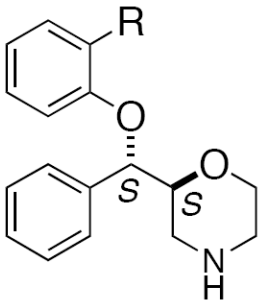

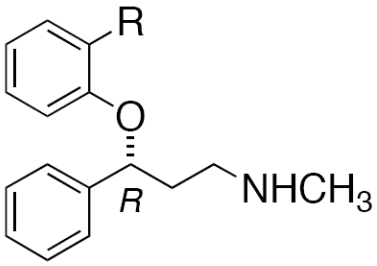

1 R = OCH_2CH_3, Reboxetine
2 R = OCH_3, MeNER
3 R = OCH_2F, FMeNER
4 R = OCH_2CH_2F, FRB
5 R = I, IPBM or INER

6 R = OCH_3, Nisoxetine
7 R = I, 2-INXT or MIPP

Figure 1.
Structures of previously reported ligands targeting NET.

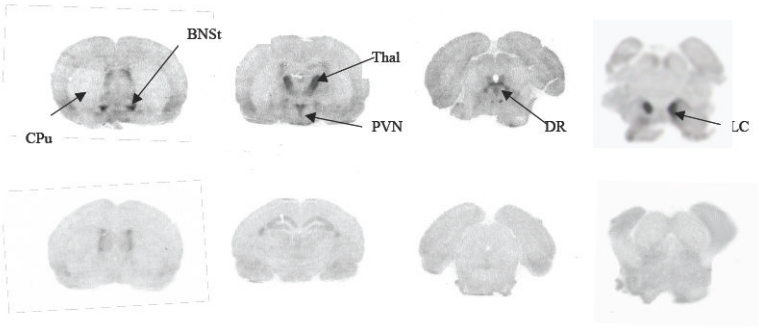

Fig.2.

Ex vivo autoradiography of rat brains at 2 hours after an iv injection of [125I]PYINXT. Top row: saline treated (control one); bottom row: nisoxetine pretreatment (10 mg/kg, 10 min prior to radiotracer administration). Abbreviations: CPu: caudate putamen; BNSt: bed nucleus of the stria terminals; DR: dorsal raphe nucleus; LC: locus coeruleus; PVN: paraventricular nucleus of the hypothalamus; Thal: thalamic nucleus.

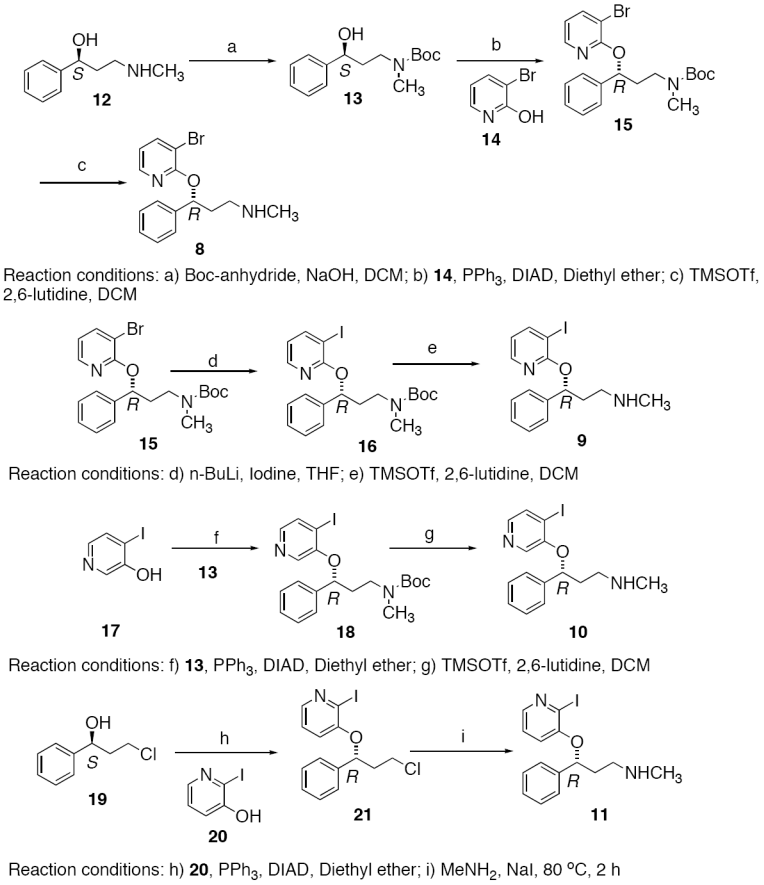

Scheme 1.
Synthesis of Compounds 8, 9, 10 and 11.

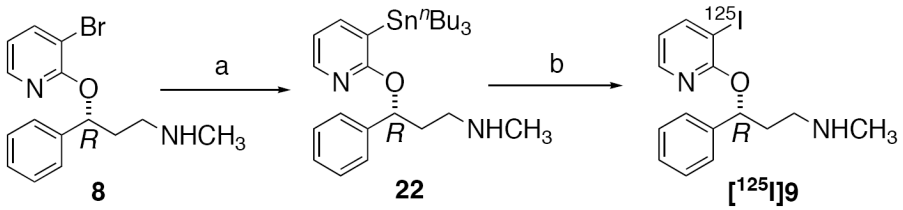

Reaction conditions: a) $(Sn^nBu_3)_2$, $Pd(PPh_3)_4$; b) $Na^{125}I/H_2O_2$, HCl

Scheme 2.
Synthesis of 22 and [125I]PYINXT.

Table 1

Inhibition constants (K_i) of NET ligands binding to homogenates prepared from LLC cells respectively expressing norepinephrine, serotonin and dopamine transporters

Compound	LLC-NET (nM)	LLC-SERT (nM)	LLC-DAT (nM)
8	5.3 ± 0.3	>5,000	>10,000
9	4.5 ± 0.7	>1,500	>10,000
10	32.5 ± 5.0	>2,000	>10,000
11	13.5 ± 2.5	>1,000	>30,000
nisoxetine	4.8 ± 1.7	>2000	>15,000

Studies were carried out with 0.08-0.08 nM [^{125}I]INXT for NET, 0.1-0.2 nM [^{125}I]IDAM for SERT and 0.1-0.2 nM [^{125}I]IPT for DAT. Values are the mean ± SEM of three determinations performed in duplicate.

Table 2

Biodistribution in rats after an IV injection of **[125I]PYINXT** (% dose/organ, average of 3 rats ± SD)

	2min	30min	60min	120 min	240 min
Blood	3.38±0.16	2.87±0.16	2.96±0.35	3.12±0.14	3.22±0.70
Heart	2.28±0.37	0.53±0.12	0.29±0.03	0.16±0.03	0.12±0.03
Muscle	24.14±13.37	13.48±2.10	15.39±1.19	9.40±0.90	5.98±0.82
Lung	10.21±1.85	3.06±0.77	1.43±0.20	0.75±0.09	0.37±0.03
Kidney	7.51±0.44	2.00±0.24	1.46±0.24	0.93±0.12	0.59±0.15
Spleen	1.04±0.51	0.76±0.21	0.56±0.03	0.26±0.03	0.12±0.02
Liver	7.37±2.01	3.48±0.08	2.91±0.28	2.43±0.03	2.08±0.15
Skin	7.09±3.01	9.13±0.69	9.55±0.74	8.33±0.81	7.12±1.76
Brain	0.54±0.08	0.46±0.00	0.33±0.03	0.16±0.01	0.07±0.01
Thyroid	0.05±0.01	0.05±0.02	0.05±0.05	0.02±0.01	0.32±0.19
Regional Brain Distribution (% dose/g ± SD)					
Cerebellum	0.41±0.02	0.28±0.00	0.18±0.03	0.09±0.01	0.04±0.00
Striatum	0.29±0.05	0.22±0.02	0.16±0.01	0.07±0.01	0.03±0.01
Hippocampus	0.28±0.06	0.26±0.02	0.20±0.01	0.11±0.01	0.04±0.01
Cortex	0.33±0.07	0.28±0.01	0.20±0.02	0.10±0.01	0.03±0.00
Remainder	0.30±0.05	0.26±0.01	0.18±0.02	0.09±0.01	0.04±0.00
Hypothalamus	0.31±0.04	0.33±0.09	0.23±0.04	0.12±0.01	0.06±0.01
Ratio vs. ST (± SD)					
Cerebellum	1.44±0.27	1.26±0.09	1.11±0.18	1.24±0.17	1.53±0.40
Striatum	1.00±0.26	1.00±0.09	1.00±0.11	1.00±0.10	1.00±0.33
Hippocampus	0.97±0.27	1.17±0.12	1.25±0.13	1.58±0.23	1.71±0.52
Cortex	1.14±0.32	1.23±0.10	1.20±0.16	1.40±0.16	1.21±0.34
Remainder	1.04±0.26	1.15±0.09	1.12±0.16	1.32±0.18	1.36±0.37
Hypothalamus	1.08±0.24	1.49±0.49	1.41±0.25	1.70±0.17	2.14±0.62